

Frequency evaluation of UTC(NMIJ) by NMIJ-Yb1 for the period MJD 61129 to MJD 61134

The secondary frequency standard NMIJ-Yb1 has been compared to UTC(NMIJ), during a measurement campaign between MJD 61129 and MJD 61134 (30 March 2026 – 4 April 2026). The Yb optical lattice clock operation covers 92.1 % of the total measurement period.

1. Results

Table 1. (a) Results of the comparison in 1×10^{-16}

Period (MJD)	$\nu(\text{UTC(NMIJ)} - \text{NMIJ-Yb1})$	Total u_A	Total u_B	$u_{A/\text{Lab}}$	$u_{B/\text{Lab}}$	u_{SecRep}	Uptime (%)
61129 - 61134	-15.0	0.16	0.84	3.1	0.54	1.7	92.1

(b) Budget of uncertainties in 1×10^{-16}

u_A: Type A uncertainty	
Yb statistics	0.16
Total	0.16
u_B: Type B uncertainty	
Yb systematics	0.83
Gravitational	0.06
Total	0.84
$u_{A/\text{Lab}}$: Type A uncertainty	
Dead time in HM – Yb	1.4
Link in HM – UTC(NMIJ)	2.8
Total	3.1
$u_{B/\text{Lab}}$: Type B uncertainty	
Microwave-optical frequency link	0.54
Total	0.54

The calibration is made using the most recently recommended value for the $6s^2 \ ^1S_0 - 6s6p \ ^3P_0$ unperturbed optical transition in the ^{171}Yb neutral atom: 518 295 836 590 863.632 Hz [1]. u_{SecRep} is the recommended uncertainty of the secondary representation [1]

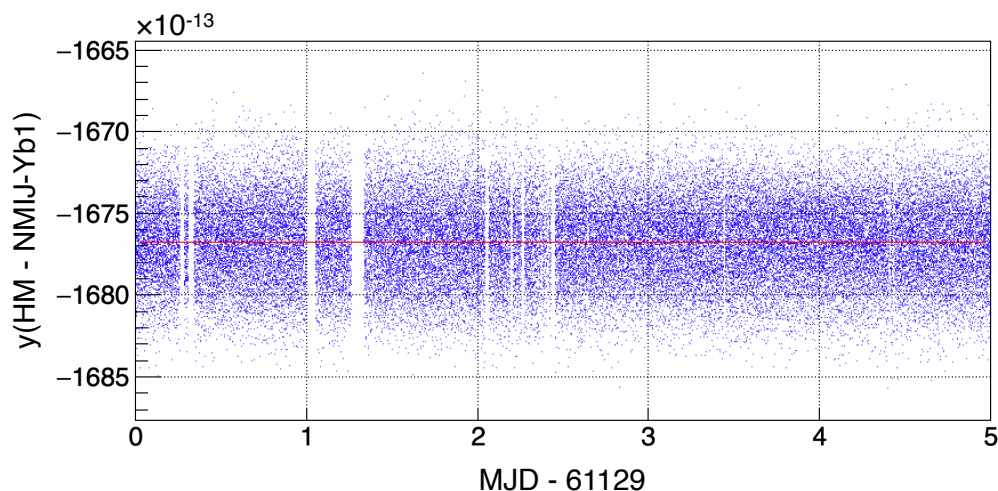


Figure 1. Data points of $y(\text{HM} - \text{NMIJ-Yb1})$ averaged over 6.8 s. The red line indicates the linear fit used to obtain the drift rate of HM (typically $-1 \times 10^{-16}/\text{d}$).

2. Systematic effects and uncertainties

Table 2. Budget of systematic effects and uncertainties for NMIJ-Yb1 [2-7] in 1×10^{-17}

Effect	Shift	Uncertainty
Lattice light	4.2	1.6
Blackbody radiation	-253.9	7.8
Density	-0.3	0.5
Second order Zeeman	-5.5	0.3
Probe light	0.4	0.9
Servo error	18.1	2.0
AOM switching	-	0.01
Line pulling	-	1
DC Stark	-	0.3
Total	-237.0	8.3
Gravitational redshift	230.8	0.6
Total (with gravitational redshift)	-6.2	8.4

For the reports submitted in November and December 2020, the total systematic uncertainty of NMIJ-Yb1 was improved to 2×10^{-16} compared with an uncertainty of 4×10^{-16} described in previous reports and Ref. [3]. A major improvement was made in the uncertainty of the lattice light shift ($\sim 3 \times 10^{-16} \rightarrow \sim 6 \times 10^{-17}$). Here we reduced the uncertainty of the magic frequency by a

factor of ~ 3 , and operated NMIJ-Yb1 with a lower trap potential depth of $\sim 200E_r$, where E_r denotes the recoil energy from a lattice photon.

For the reports submitted in August 2021 and after that, the total systematic uncertainty of NMIJ-Yb1 was improved to 1×10^{-16} . The uncertainty of the blackbody radiation shift was reduced from $\sim 2 \times 10^{-16}$ to $\sim 1 \times 10^{-16}$ by (a) reducing the temperature inhomogeneity of a vacuum chamber for trapping atoms, (b) inserting an aperture to reduce the solid angle of a window heated at ~ 200 °C, and (c) reevaluating the contributions from hot vacuum components (e.g., the heated window and atomic oven) with a Monte Carlo ray-tracing analysis.

For the reports submitted in April 2023 and after that, the evaluation of the DC Stark shift was included. The uncertainty of the blackbody radiation shift was slightly improved by using measured surface roughness of the vacuum chamber in the Monte Carlo ray-tracing analysis. The uncertainty of the probe light shift was increased from $\sim 3 \times 10^{-18}$ to $\sim 1 \times 10^{-17}$, taking account of the effect of small residual ellipticity of the probe light which has recently been investigated [4]. A paper describing the improved uncertainty evaluation of NMIJ-Yb1 after November 2020 has been published [5].

For the reports in March 2026 and after that, the total systematic uncertainty of NMIJ-Yb1 was improved to $\sim 8 \times 10^{-17}$. The uncertainty of the lattice light shift was reduced from $\sim 5 \times 10^{-17}$ to $\sim 2 \times 10^{-17}$ by operating axially sideband-cooled atoms in a lower trap depth ($\sim 70E_r$) [6]. The uncertainty of the magic frequency was also reduced by a factor of ~ 2 compared with that described in Ref. [5], by performing an interleaved measurement with sideband cooling. Since our previous evaluation of the density shift [5] was done without sideband cooling, the density shift was also reevaluated by an interleaved measurement. To reduce the uncertainty of the blackbody radiation shift, we installed an in-vacuum temperature sensor mounted on a glass tube. The evaluation result of the blackbody radiation shift will be reported in the future [6]. The DC Stark shift due to the glass tube was estimated as $< 3 \times 10^{-18}$ based on a finite element analysis. The uncertainty arising from the AOM (acousto-optic modulator) switching was reduced to less than 1×10^{-19} by stabilizing the optical pass length including the AOM.

The gravitational redshift was calculated with respect to the conventionally adopted reference potential $W_0 = 62\,636\,856.0 \text{ m}^2/\text{s}^2$. For the reports submitted in July 2022 and after that, the uncertainty of the gravitational redshift was improved from 6×10^{-17} to 6×10^{-18} using the geopotential value of NMIJ-Yb1 measured by Geospatial Information Authority of Japan [7].

3. Frequency comparison

Table 3. Frequency correction and uncertainty for $\nu(\text{HM} - \text{NMIJ-Yb1})$ due to the dead time in HM –

Yb in 1×10^{-17}

Effect	Correction	Uncertainty
Maser noise model	-	12.9
Linear drift	-0.5	4.2
Total	-0.5	13.5

For the report submitted in April 2023 and after that, the frequency of NMIJ-Yb1 was compared with HM (clock code: 1405012) instead of UTC(NMIJ) using an optical frequency comb. A beat frequency between a laser locked to an ultra-stable cavity and the comb was counted. The frequency of the ultra-stable laser was shifted by an AOM and stabilized to the clock transition in ^{171}Yb atoms trapped in an optical lattice. The frequency of the AOM was then combined with the beat frequency to compute $\gamma(\text{HM} - \text{NMIJ-Yb1})$. For the report submitted in January 2025 and after that, we measured the frequency difference between HM and UTC(NMIJ) by a time interval counter to yield the frequency difference between UTC(NMIJ) and NMIJ-Yb1.

The uncertainty $u_{\text{B/Lab}}$ arose from a microwave-optical frequency link. For the reports submitted in November 2020 and after that, this uncertainty was improved to 1.0×10^{-16} compared with an uncertainty of 2.2×10^{-16} described in previous reports and Ref. [3]. The previous uncertainty was mainly caused by frequency multiplication of a 10 MHz signal from UTC(NMIJ). Here we reduced this uncertainty to low 10^{-17} by carefully stabilizing the temperature of a frequency multiplier. The present $u_{\text{B/Lab}}$ uncertainty was limited by phase variations of the 10 MHz signal that occurred during its transmission through a coaxial cable.

For the reports in March 2026 and after that, $u_{\text{B/Lab}}$ was improved to 5.4×10^{-17} by employing a coaxial cable with a smaller temperature dependence [8].

The uncertainty $u_{\text{A/Lab}}$ arose from (i) the dead time in the comparison between NMIJ-Yb1 and HM and (ii) measurement noise of the time interval counter for the frequency difference between HM and UTC(NMIJ). (i) The dead time uncertainty was estimated using a method described in Ref. [9]. For this estimation, we derived a maser noise model from the measured stability of HM against NMIJ-Yb1. The model includes a white phase modulation of $2 \times 10^{-12} / (\tau / \text{s})$, a white frequency modulation (FM) of $1 \times 10^{-13} / (\tau / \text{s})^{1/2}$, a flicker FM of 5×10^{-16} , a random walk FM of $2 \times 10^{-30} (\tau / \text{s})^{1/2}$. The $u_{\text{A/Lab}}$ also includes the uncertainty of a frequency correction resulting from the dead time based on the linear drift of HM. The drift rate of HM was determined by fitting the measured data of $\gamma(\text{HM} - \text{NMIJ-Yb1})$ with a linear function (see Fig. 1). (ii) The measurement noise of the time interval counter was estimated by $1.2 \times 10^{-10} / (\tau / \text{s})$.

References

- [1] “Recommended values of standard frequencies for applications including the practical realization of the metre and secondary representations of the definition of the second,” BIPM publication, approved by CCTF September 2025,
https://www.bipm.org/documents/20126/69375133/171Yb_518THz_2021.pdf/283dca33-4dac-f309-671e-577af2a62fc1
- [2] T. Kobayashi, D. Akamatsu, Y. Hisai, T. Tanabe, H. Inaba, T. Suzuyama, F.-L. Hong, K. Hosaka, and M. Yasuda, “Uncertainty Evaluation of an ^{171}Yb Optical Lattice Clock at NMIJ,” *IEEE Trans. Ultrason., Ferroelectr., Freq. Control* **65**, 2449-2458 (2018).
- [3] T. Kobayashi, D. Akamatsu, K. Hosaka, Y. Hisai, M. Wada, H. Inaba, T. Suzuyama, F.-L. Hong, and M. Yasuda, “Demonstration of the nearly continuous operation of an ^{171}Yb optical lattice clock for half a year,” *Metrologia* **57**, 065021 (2020).
- [4] V. I. Yudin, A. V. Taichenachev, O. N. Prudnikov, M. Yu. Basalae, V. G. Pal’chikov, M. von Boehn, T. E. Mehlstäubler, and S. N. Bagayev, “Probe-Field-Ellipticity-Induced Shift in an Atomic Clock,” *Phys. Rev. Applied* **19**, 014022 (2023).
- [5] T. Kobayashi, A. Takamizawa, D. Akamatsu, A. Kawasaki, A. Nishiyama, K. Hosaka, Y. Hisai, M. Wada, H. Inaba, T. Tanabe, and M. Yasuda, “Search for Ultralight Dark Matter from Long-Term Frequency Comparisons of Optical and Microwave Atomic Clocks,” *Phys. Rev. Lett.* **129**, 241301 (2022).
- [6] T. Kobayashi *et al.*, in preparation.
- [7] M. Nakashima, S. Fukaya, T. Toyofuku, K. Ochi, and K. Matsuo, “Determination of geopotential values at the optical lattice clocks based on geodetic approaches,” Japan Geoscience Union Meeting, SGD02-14 (2022).
- [8] M. Wada and H. Inaba, “Femtosecond-comb based 10 MHz-to-optical link with uncertainty at the 10^{-18} level,” *Metrologia* **59**, 065005 (2022).
- [9] D.-H. Yu, M. Weiss, and T. E. Parker, “Uncertainty of a frequency comparison with distributed dead time and measurement interval offset,” *Metrologia* **44**, 91-96 (2007).